Systematics of the Photoemission Spectral Function of Cuprates: Insulators and Hole- and Electron-Doped Superconductors

C. Kim,[1] P. J. White,[1] Z.-X. Shen,[1] T. Tohyama,[2] Y. Shibata,[2,*] S. Maekawa,[2] B. O. Wells,[3,†] Y. J. Kim,[3] R. J. Birgeneau,[3] and M. A. Kastner[3]

[1]*Department of Applied Physics and Stanford Synchrotron Radiation Laboratory, Stanford University, Stanford, California 94305*

[2]*Institute for Materials Research, Tohoku University, Sendai 980-77, Japan*

[3]*Department of Physics, Massachusetts Institute of Technology, Cambridge, Massachusetts 02139*

(Received 26 August 1997)

Angle-resolved photoemission studies on $Sr_2CuO_2Cl_2$ at a temperature below its Néel temperature reveal detailed momentum dependent line shape changes as a function of wave vector. While a sharp quasiparticlelike peak is observed near $(\pi/2, \pi/2)$, broad peaks are observed near $(\pi, 0)$. Additional second and third neighbor hopping terms must be added to the t-J Hamiltonian to account for both the dispersion and the line shape. It is found that this Hamiltonian can be used to explain the measured momentum dependent spectral function for hole-doped materials, both underdoped and overdoped, as well as electron-doped materials. [S0031-9007(98)06100–6]

PACS numbers: 71.27.+a, 78.20.Bh, 79.60.Bm, 79.60.–i

The copper oxides are unusual in that the undoped materials are antiferromagnetic insulators, but doping converts them into high-T_c superconductors. Knowledge of the electronic structure is a critical first step toward a microscopic understanding of this fascinating behavior, and angle-resolved photoemission spectroscopy (ARPES) experiments [1], together with band structure calculations [2] and numerical simulations based on many-body models [3], have been one of the primary sources of this knowledge.

Recent ARPES experiments on insulating $Sr_2CuO_2Cl_2$ [4,5] have stimulated a number of theoretical studies of a single hole in an antiferromagnetic background [6–12]. These show that the t-J model (t and J are the nearest-neighbor hopping matrix element and antiferromagnetic exchange, respectively) can quantitatively explain the observed dispersion of the energy E(**k**) from $\mathbf{k} = (0, 0)$ to (π, π) with a total bandwidth of about $2.2J$. However, the model does not explain the data near $\mathbf{k} = (\pi, 0)$; the nearest-neighbor t-J model predicts that the energies at $(\pi, 0)$ and $(\pi/2, \pi/2)$ are very similar, but the experimental energy at $(\pi, 0)$ is higher than that at $(\pi/2, \pi/2)$ by about $2J$. This discrepancy has led to intense theoretical activity [6–13], and recent work shows that it may be resolved by introducing hopping to second and third nearest neighbors, that is, by using a t-t'-t''-J model [7–12].

While the dispersion of the lowest energy ARPES peak helps to characterize the holes, the doping and momentum dependences of the ARPES line shape also contain important information. For example, the spectral shape at $(\pi, 0)$ rapidly changes from a broad edgelike feature for underdoped samples to a sharp peak for overdoped samples, even though the T_c difference is not very large [14]; this rapid change of the line shape is correlated with the size of the superconducting gap. Hence, an understanding of the line shape evolution with doping may provide clues about the pairing mechanism as well as the dependence of the electronic structure on hole concentration.

Before addressing the superconductor, one must first clarify how the line shape evolves with **k** in the undoped material. To do this, one needs measurements of the prototype material $Sr_2CuO_2Cl_2$ at low enough temperature that detailed line shape information can be obtained. Previous measurements have been limited to $T > 300$ K because of electrostatic charge accumulation on the sample. We have overcome this problem [15], allowing measurements at 150 K that reveal better resolved line shapes. We find that the spectrum near $(\pi/2, \pi/2)$ consists of a single relatively sharp peak, while the spectra along Γ-$(\pi, 0)$ are very broad and consist of at least two peaks separated by about 0.4 eV.

In order to interpret these new results we have performed exact diagonalization studies using both the t-J and the t-t'-t''-J models. The latter gives a much better account of the data than the former, yielding a sharp peak at $(\pi/2, \pi/2)$ and a very broad structure near $(\pi, 0)$. Encouraged by this, we have performed further numerical studies to determine the doping dependence predicted by the t-t'-t''-J model. The model satisfactorily describes the observed sharpening of the peak at $(\pi, 0)$ with increased doping, and can also explain the difference in the spectra near $(\pi, 0)$ of the hole- and electron-doped superconductors. These new findings show that t' and t'' are essential not only for the doping dependent dispersion of the lowest energy peak [11], but also for the systematic evolution of the spectral line shape.

Experiments were performed at beam line V of the Stanford Synchrotron Radiation Laboratory. $Sr_2CuO_2Cl_2$ single crystals [16], which were oriented prior to the experiments were cleaved *in situ*. The base pressure was better than 5×10^{-11} torr. With 22.4 eV photons, the

total energy resolution was typically 70 meV, and the angular resolution was $\pm 1°$. The spectra from $Sr_2CuO_2Cl_2$ reported here were all taken at 150 K and within 6 hours after the initial cleave.

Figure 1 shows ARPES data taken at 150 K, well below the Néel temperature of 256 K [4]. The number on each spectrum shows the **k** position in units of π/a where $a = 3.967$ Å at 300 K is the Cu-O-Cu bond length. Panel (a) shows a cut along the Γ-(π, π) direction. Along this direction the low energy peak, which we refer to as the quasiparticle peak, moves by about 0.3 eV toward the low excitation energy side, reaches its minimum at $(\pi/2, \pi/2)$, and then folds back with a rapid reduction of the intensity. This behavior is the same as that reported earlier [4]. However, compared to the earlier measurements the peaks near $(\pi/2, \pi/2)$ are relatively sharp, reminiscent of those resulting from quasiparticles, on top of a flat "background" on the higher energy side.

The spectra along the Γ-$(\pi, 0)$ cut at 150 K, in panel (b), show strong peaklike features, whereas the spectra at 350 K are much broader. However, the dispersion is similar to that reported earlier. The spectral weight has its maximum at around $(2\pi/3, 0)$, and as **k** is increased further toward $(\pi, 0)$, the low energy features are suppressed. Notice that the peaks along this cut show a shoulder at about 0.4 eV below the primary peak. This is most obvious in the spectrum at $(\pi/2, 0)$. It is interesting to note that string resonance states have been predicted at this energy [3]. The tick marks in Fig. 1 indicate the centroids of the two features, determined by fitting the spectra with a function that accounts for the instrumental resolution and lifetime broadening.

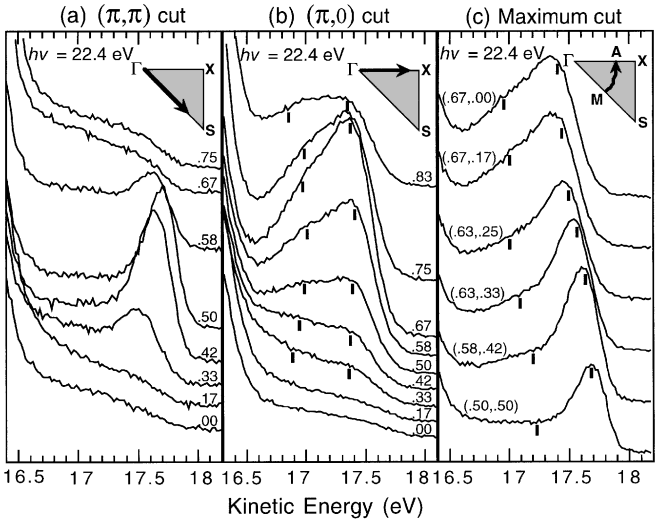

FIG. 1. ARPES data for $Sr_2CuO_2Cl_2$ at 150 K. Spectral intensities within a panel are correct relative to one another, but not between panels. (a) The spectra taken along the Γ-(π, π) direction (see inset). The number on each spectrum represents the momentum in units of π/a where a is the Cu-O-Cu bond length. (b) Spectra taken along the Γ-$(\pi, 0)$ direction. The spectral intensity is highest on an arc connecting $(\pi/2, \pi/2)$ and $(2\pi/3, 0)$. (c) Spectra taken on this maximum cut. The tick marks in panels (b) and (c) are guides to the eye for the centroids of the features. The positions are determined by curve fitting.

The spectral weight has its maximum on an arc connecting the $(\pi/2, \pi/2)$ and $(2\pi/3, 0)$ points. Panel (c) shows the spectra taken along this "maximum" cut. The 0.4 eV feature is suppressed as **k** is varied from $(2\pi/3, 0)$ to $(\pi/2, \pi/2)$, eventually leaving only the flat background mentioned above. The total dispersion along the maximum cut is about 0.3 eV, while that along the Γ-$(\pi, 0)$ cut is less than 0.1 eV. The separation between the primary peak and the shoulder remains approximately constant.

Figure 2 compares the spectra for $Sr_2CuO_2Cl_2$ with those of $Bi_2Sr_2CaCu_2O_{8+\delta}$ and $Nd_{1.85}Ce_{0.15}CuO_4$ (from King *et al.* [17]). We show the $Sr_2CuO_2Cl_2$ spectra at $(\pi/2, \pi/2)$, $(\pi/2, 0)$, and $(\pi, 0)$ in Fig. 2(a). As **k** changes from $(\pi/2, \pi/2)$ to $(\pi/2, 0)$, the spectra show not only that the quasiparticle peak moves toward higher excitation energy as reported earlier [4], but also that the relative intensity of the shoulder grows. At the $(\pi, 0)$ point the quasiparticle peak is strongly suppressed. This evolution of the line shape is similar to that of underdoped $Bi_2Sr_2CaCu_2O_{8+\delta}$ as shown in Fig. 2(b). The peak at the Γ-(π, π) Fermi crossing is sharp while the peak at $(\pi, 0)$ is broad and suppressed. In the overdoped sample [Fig. 2(c)], the peak at $(\pi, 0)$ moves closer to the Fermi energy and becomes sharp with increased intensity while the line shape on the Γ-(π, π) cut remains more or less the same as in the underdoped sample.

Summarizing the results, upon hole doping from the insulator to the overdoped superconductor, the quasiparticle peak at $(\pi, 0)$ (i) moves toward the Fermi energy, (ii) becomes sharper, and (iii) increases in intensity. In contrast, doping has relatively little effect on the peak near $(\pi/2, \pi/2)$. The data for $Nd_{1.85}Ce_{0.15}CuO_4$ in Fig. 2(d) show that the electron-doped material is different. The

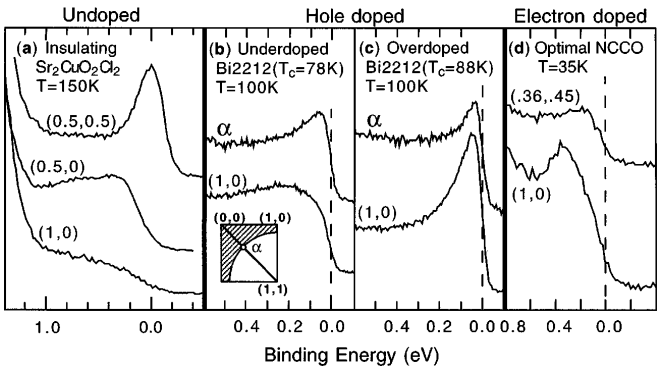

FIG. 2. Comparison of spectra of (a) $Sr_2CuO_2Cl_2$ at $(\pi, 0)$, $(\pi/2, 0)$, and $(\pi/2, \pi/2)$ with those at $(\pi, 0)$ and at the Γ-(π, π) Fermi crossing (see inset) for (b) underdoped and (c) overdoped $Bi_2Sr_2Ca_2Cu_2O_{8+\delta}$, and (d) $Nd_{1.85}Ce_{0.15}CuO_4$ (from Ref. [17]). The data acquisition temperatures are shown in the figure.

peak at $(\pi, 0)$ is at a considerably higher excitation energy than that for the hole-doped materials. The experimental resolution is not high enough to reveal details of the line shape.

We next present an interpretation of these results based on exact diagonalization studies. We focus on the evolution of the global features which are not affected by the finite cluster size used in these studies. In Fig. 3, we compare the results using the t-J and t-t'-t''-J models for various levels of hole doping. Parameter values are set to be $t = 0.35$ eV, $t' = -0.12$ eV, $t'' = 0.08$ eV, and $J = 0.14$ eV. These parameters describe the measured dispersion relation in $Sr_2CuO_2Cl_2$ adequately and are consistent with other calculations and measurements. In particular, the ratio t'/t is consistent with recent measurements that give the ratio of second to first neighbor exchange $J'/J \sim (t'/t)^2 \sim 0.1$ [18]. On the one hand, comparing the results from the calculation for the insulator in Fig. 3(a) with the experimental data in Fig. 2(a), one sees that the t-J model can explain neither the line shape nor the dispersion of the experimental data near $(\pi, 0)$. On the other hand, the t-t'-t''-J model reproduces the experimental evolution of the quasiparticle peak. In particular, one sees from Fig. 3(b) that as $\mathbf{k}$ is varied from $(\pi/2, \pi/2)$ to $(\pi, 0)$, the quasiparticle peak moves toward higher excitation energy and is strongly suppressed. Also note that the relative intensity of the second (higher energy) feature increases. Since the t-J model gives a larger quasiparticle weight at $(\pi, 0)$ than the t-t'-t''-J model, it appears that the t' and t'' terms are responsible for the suppression of the quasiparticle weight observed experimentally.

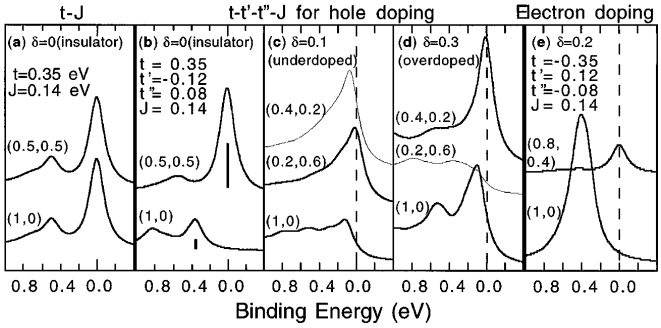

FIG. 3. Single particle spectral functions of t-J and t-t'-t''-J. Calculations are performed on the 16- and 20-site clusters for the insulating and dopes cases, respectively. The δ functions are convolved with a Lorentzian broadening of 0.10 eV. The parameters used in the calculation are shown in the figure. The binding energy is measured from the energy of the first ionization state in the photoemission process. (a) t-J and (b) t-t'-t''-J results on half filling. The vertical bars in (b) denote the calculated weight of $|\Psi_{\mathbf{k}}^{\text{Néel}}\rangle$. ARPES data at α and $(\pi, 0)$ from under- and overdoped $Bi_2Sr_2Ca_2Cu_2O_{8+\delta}$ can be compared with the single particle spectral functions (c) at $(\pi/5, 3\pi/5)$ and $(\pi, 0)$ for $\delta = 0.1$, and (d) at $(2\pi/5, \pi/5)$ and $(\pi, 0)$ for $\delta = 0.3$. The quasiparticle peak at $(\pi/5, 3\pi/5)$ for $\delta = 0.3$ appears above the Fermi level, i.e., in the inverse photoemission process. (e) Numerical results ($\delta = 0.2$) on electron doping.

One can understand this as follows: For the chosen values of t' and t'' the energy of the Néel state with a hole, $|\Psi_{\mathbf{k}}^{\text{Néel}}\rangle$ is relatively large for $\mathbf{k} = (\pi, 0)$, reducing the one-hole-Néel-state character of the final state associated with the quasiparticle peak. Since the initial state is antiferromagnetically ordered, the photoemission spectral weight is expected to be proportional to the one-hole-Néel-state character of the final state, $(|\langle f|c_{k\sigma}|i\rangle|^2 = |\langle f|c_{k\sigma}|AF\rangle|^2 \sim |\langle f|\Psi_{\mathbf{k}}^{\text{Néel}}\rangle|^2)$. The vertical bars in Fig. 3(b) denote the calculated weight of $|\Psi_{\mathbf{k}}^{\text{Néel}}\rangle$ in the eigenstate corresponding to the quasiparticle. Note that the bar heights are roughly proportional to the weight of the quasiparticle peak resulting from the full t-t'-t''-J model calculation. The fact that the feature at $(\pi, 0)$ in the t-t'-t''-J calculation is weaker than the corresponding one in the t-J calculation means that for a hole with $\mathbf{k} = (\pi, 0)$ the interplay of t' and t'' with t and J causes a further weakening of the antiferromagnetic spin correlations.

Figures 3(c) and 3(d) show the t-t'-t''-J results on the doping dependence of the spectral function for a $\sqrt{20} \times \sqrt{20}$-site cluster, using the same t' and t'' values as for $Sr_2CuO_2Cl_2$. This is justified since band calculations show similar Fermi surface topologies for $Sr_2CuO_2Cl_2$ [19] and $Bi_2Sr_2CaCu_2O_8$ [20]. Here we focus on the global evolution of the spectral function, which is possible even with the limited momenta available in the small cluster. The spectrum at $(\pi/5, 3\pi/5)$ can be compared [11,21] with the experimental data at the point α for the underdoped case in Fig. 2(b). We see that the theoretical peak at $(\pi/5, 3\pi/5)$ is sharp while the spectrum at $(\pi, 0)$ is broad. At $\delta = 0.3$, the peak at $(\pi/5, 3\pi/5)$ moves above the Fermi energy. For $\delta = 0.3$ the peak at $(2\pi/5, \pi/5)$ is again sharp as in the $\delta = 0.1$ case. On the other hand, the spectrum at $(\pi, 0)$ shows a significant doping dependence, with a sharp feature at the lowest excitation energy with increased spectral weight compared to $\delta = 0.1$. This behavior is consistent with the experimental data in Fig. 2. We note that the intensity near the Fermi level increases with δ because the spectral weight, which was concentrated at a high energy for the undoped case, moves to lower energies as δ increases. We also note that the position of the suppressed quasiparticle peak at $(\pi, 0)$ shifts to near the Fermi level with doping, as previously shown by Eder *et al.* [11].

The great breadth of the quasiparticle peak at $(\pi, 0)$ for $\delta = 0.1$ is caused by the reduction of the quasiparticle weight, which may come from two alternative but related sources: there could be larger phase space for decay of quasiparticles because of strong coupling of the photo hole to collective magnetic excitations near $\mathbf{q} = (\pi, \pi)$ [22]. The Fermi surface topology is changed by the inclusion of t' and t'' [23] in a way that enhances this coupling. Alternatively, the same mechanism of the coupling between

charge motion and spin background discussed above for the undoped case could be more effective in the lightly doped material, although the spin correlation length is expected to be short for $\delta = 0.1$. Both of these mechanisms are likely to have less importance for the overdoped case, in which the magnetic correlations are expected to be weak [24]. Our interpretation of the data using the t-t'-t''-J model is different from that of Laughlin [13] where the $(\pi, 0)$ behavior is attributed to the spin-charge separation in a nonordered state at elevated temperatures. Nonetheless, the central idea in the two interpretations is similar. The $(\pi, 0)$ behavior is a manifestation of the reduction of magnetic order, whether resulting from t' and t'' on the one hand, or temperature, on the other.

In our calculations electron doping is qualitatively different from hole doping. All of the hopping terms have opposite signs for electron and hole doping when the three-band Hubbard model is mapped onto the t-t'-t''-J model [25], and the signs of t' and t'' are of crucial importance for the coupling of the charge motion to the spin background [25]. One sees from Fig. 3(e) that the quasiparticle spectral weight at $(\pi, 0)$ is very large compared to the hole-doped case. For electron doping t' and t'' appear to enhance the antiferromagnetic correlations near half filling [25]. Therefore, the Néel-like state becomes more stable, unlike the hole-doped case, resulting in large quasiparticle weight. We also note that the binding energy of the $(\pi, 0)$ peak is larger than that for the hole-doped case. This is due to a band structure effect that makes the energy of the band near $(\pi, 0)$ higher in contrast to the hole-doped case where the band near $(\pi, 0)$ is flat. While the dispersion is consistent with the experimental data, shown in Fig. 2(d), the resolution of the experimental data is not high enough to compare with our prediction of the line shape. Hence, high resolution measurements of the spectra on the underdoped n-type material will provide a crucial test of the theory.

In conclusion, introduction of second and third neighbor hopping provides a description of both the dispersion and the line shape of the ARPES data for $Sr_2CuO_2Cl_2$. Calculated spectra using the t-t'-t''-J Hamiltonian for hole- and electron-doped layered copper oxides are in qualitative agreement with experiment. These longer range hopping terms play an important role in the coupling of the charge-carrier motion to the spin background. Moreover, this work confirms the importance of the antiferromagnetic correlations throughout the superconducting region of the phase diagram [24].

This work was supported by the U.S. DOE, Office of Basic Energy Science, Division of Material Science, NEDO, and the Ministry of Education, Science and Culture of Japan. Stanford Synchrotron Radiation Laboratory is operated by the U.S. DOE, Office of Basic Energy Sciences, Division of Chemical Sciences. The computation was performed on the supercomputers at ISSP, University of Tokyo, and IMR, Tohoku University. Work at MIT has been supported primarily by the MRSEC Program of the National Science Foundation under Award No. DMR 94-00334.

*On leave from Department of Applied Physics, Nagoya University, Nagoya 464-01, Japan.

†Present address: Boeing Aerospace - Phantom Works m/s 531/C243, 5000 East McDowell Road, Mesa, AZ 85215.

[1] Z.-X. Shen *et al.*, Phys. Rep. **253**, 1 (1995).
[2] W. E. Pickett, Rev. Mod. Phys. **61**, 433 (1989).
[3] E. Dagotto, Rev. Mod. Phys. **66**, 763 (1994), and references therein.
[4] B. O. Wells *et al.*, Phys. Rev. Lett. **74**, 964 (1995).
[5] S. LaRosa *et al.*, Phys. Rev. B **56**, R525 (1997).
[6] A. Nazarenko *et al.*, Phys. Rev. B **51**, 8676 (1995).
[7] B. Kyung *et al.*, Phys. Rev. B **54**, 10 125 (1996).
[8] T. Xiang *et al.*, Phys. Rev. B **54**, R12 653 (1996).
[9] V. I. Belinicher *et al.*, Phys. Rev. B **54**, 14 914 (1996).
[10] T. K. Lee *et al.*, Phys. Rev. B **55**, 5983 (1997).
[11] R. Eder *et al.*, Phys. Rev. B **55**, R3414 (1997).
[12] P. W. Leung *et al.*, cond-mat/9702016.
[13] R. B. Laughlin, Phys. Rev. Lett. **79**, 1726 (1997).
[14] P. J. White *et al.*, Phys. Rev. B **54**, R15 669 (1996).
[15] The resistance of the contact between the sample and the substrate was large enough to cause charging problems in our previous experiments. Reducing this contact resistance has made measurements possible down to 150 K.
[16] L. L. Miller *et al.*, Phys. Rev. B **41**, 1921 (1990).
[17] D. M. King *et al.*, Phys. Rev. Lett. **70**, 3159 (1993); R. O. Anderson *et al.*, Phys. Rev. Lett. **70**, 3163 (1993).
[18] F. C. Chou *et al.*, Phys. Rev. Lett. **78**, 535 (1997).
[19] O. K. Andersen *et al.*, J. Phys. Chem. Solids **56**, 1573 (1995); D. L. Novikov *et al.*, Phys. Rev. B **51**, 6675 (1995).
[20] S. Massidda *et al.*, Physica (Amsterdam) **152C**, 251 (1988).
[21] T. Tohyama *et al.*, J. Phys. Soc. Jpn. **65**, 1902 (1996).
[22] Z.-X. Shen *et al.*, Phys. Rev. Lett. **78**, 1771 (1997).
[23] T. Tanamoto *et al.*, J. Phys. Soc. Jpn. **62**, 717 (1993).
[24] K. Yamada *et al.*, Phys. Rev. B **57**, 6151 (1998).
[25] T. Tohyama *et al.*, Phys. Rev. B **49**, 3596 (1994).